A methodology to develop simplified kinetic schemes for detonation simulations

F. Veiga-Lopez, A. Chinnayya, J. Melguizo-Gavilanes
Institut Pprime, UPR 3346 CNRS, ISAE–ENSMA
86961 Futuroscope-Chasseneuil Cedex, France

1 Introduction

One of the main challenges in combustion modeling is the integration of the chemistry. For illustrative purposes, a detailed mechanism for a typical hydrocarbon fuel used in transportation may include hundreds of species and thousands of reactions [1]. Significant efforts have been made to develop reduction techniques aiming to keep their predictive capabilities intact while minimizing the number of species transported such as quasi-steady state, directed graph, manifold and genetic algorithms methods [2–4] or simpler systematic approaches based on error metrics [5]. The turbulent combustion community has spearheaded most of these efforts likely driven by industrial needs [6,7], both in stationary and mobile energy conversion systems, so that more fuel efficient and less polluting alternatives can be devised.

The detonation community has lacked such drivers and has been satisfied with a mostly qualitative understanding of the phenomenon given by the simplest descriptions of the chemistry; this is due in part to the very stringent resolution requirements to adequately resolve multidimensional detonation fronts. In actuality, when predictions are needed for limiting behaviors (i.e., detonability limits, detonation initiation/diffraction and quenching) experimental databases continue to be the most reliable source [8], although some success has been achieved recently when coupling inviscid hydrodynamic solvers with H_2-O_2 detailed kinetics (9 species/21 reactions) [9, 10].

Integrating more complex fuels remains prohibitively expensive, hence, a good compromise would be to develop simplified kinetic schemes (extensions to the one-step model) that are capable of reproducing quantitatively the limiting behaviors mentioned above. Some past and recent efforts on simplified modeling for detonation applications include two- to five-step schemes developed with varying degrees of sophistication [11–14]. One common feature present in detonation initiation, propagation and diffraction is that their fronts are observed to be curved. Conventional fitting procedures, however, rely on using the laminar planar ZND structure hoping to reproduce the complex thermodynamic changes and associated chemical rates in the induction zone of multidimensional detonations. As it will be discussed below, kinetic schemes fitted in such a way (or variations thereof such as targeting constant volume induction times over a temperature

and pressure range of interest) not only fail at predicting the minimum reactive layer height for detonation propagation under yielding confinement [9] but also at capturing the simplest extension to the ZND model, i.e., slightly-curved/quasi-steady detonation waves, the so called $D - \kappa$ curves.

It is only natural to expect that fitting the rates of simplified schemes to capture the critical curvatures predicted by detailed mechanisms would result in simplified kinetics that reproduce more closely the expected chemical rates in the reaction zone at sub-D_{CJ} conditions. Next, we present a methodology in which $D - \kappa$ curves obtained with detailed kinetics are used as the fitting target.

2   Physical model

2.1   Governing equations

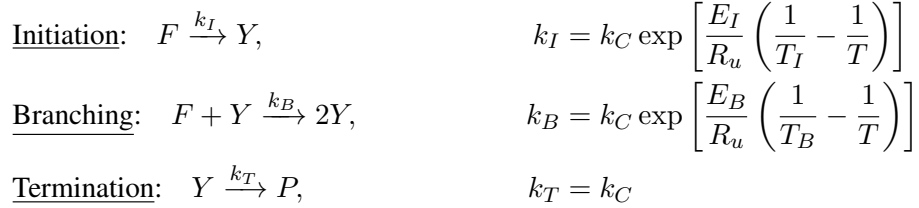The flow is described by the compressible reactive Euler equations including curvature losses.

$$\frac{\mathrm{d}\rho}{\mathrm{d}t} = -\rho\frac{(\dot{\sigma} - w(1 - \eta)\alpha)}{\eta},$$

$$\frac{\mathrm{d}w}{\mathrm{d}t} = w\frac{(\dot{\sigma} - w\alpha)}{\eta},$$

$$\frac{\mathrm{d}p}{\mathrm{d}t} = -\rho w^2\frac{(\dot{\sigma} - w\alpha)}{\eta}, \qquad\qquad \dot{\sigma} = \sum_{k=1}^{N}\left(\frac{\overline{W}}{W_k} - \frac{h_k}{c_p T}\right)\frac{\mathrm{d}Y_k}{\mathrm{d}t},$$

$$\frac{\mathrm{d}Y_k}{\mathrm{d}t} = \frac{W_k\dot{\omega}_k}{\rho}, \quad (k = 1, ..., N) \qquad\qquad \alpha = \frac{1}{A}\frac{\mathrm{d}A}{\mathrm{d}x} = \kappa\left(\frac{D}{w} - 1\right).$$

where, ρ, w, p, and t are the mixture density, axial velocity in the wave-attached frame, pressure, and time, respectively. The mass fraction, molecular weight and net production/consumption rate per unit mass of species k are given by Y_k, W_k and $\dot{\omega}_k$. Here $\eta = 1 - M^2$ is the sonic parameter and $M = w/a_f$ is the Mach number relative to the leading shock computed using the frozen speed of sound, a_f. $\dot{\sigma}$ is the thermicity, α the axial area change, $\overline{W}$ is the mean molar mass of the mixture, c_p the mixture specific heat at constant pressure, and h_k is the specific enthalpy of species k. Finally, κ is the curvature of the wave front given by $2/R_c$ for spherical waves, and $1/R_c$ for cylindrical waves with R_c being the local radius of curvature; see [15] for additional details. It can be readily shown that setting $\alpha = 0$ reverts the formulation to the ideal case included in Browne et al. [16]. The implementation in the Shock and Detonation Toolbox (SDT) [16] only entails adding the terms containing α, making it rather straight forward, and most importantly, allowing us to investigate arbitrary chemical mechanisms written in Cantera format [17] (i.e., *.cti* files).

2.2   Chemical modeling

The chemistry is modeled using the same strategy presented in Taileb et al. [9], namely, chemical schemes of increasing complexity (single-step, three-step chain-branching and detailed kinetics [18]). For completeness, we briefly describe the most salient features and assumptions made in the simplified schemes. In the single-step model, the fuel, F, is directly converted into products following a single irreversible Arrhenius

reaction, $F \rightarrow P$, occurring at a rate $k = A_s \exp(-E_a/R_u T)$. In the three-step chain-branching model, we account for *initiation*, *branching* and *termination* steps that mimic, respectively, the initial thermally neutral decomposition of the fuel (F) to produce active radicals (Y) at rate k_I, the subsequent abrupt increase of the radical pool at rate k_B, and their final conversion into products (P) at rate k_T accompanied by heat release.

$$\text{Initiation:} \quad F \xrightarrow{k_I} Y, \qquad\qquad k_I = k_C \exp\left[\frac{E_I}{R_u}\left(\frac{1}{T_I} - \frac{1}{T}\right)\right]$$

$$\text{Branching:} \quad F + Y \xrightarrow{k_B} 2Y, \qquad\qquad k_B = k_C \exp\left[\frac{E_B}{R_u}\left(\frac{1}{T_B} - \frac{1}{T}\right)\right]$$

$$\text{Termination:} \quad Y \xrightarrow{k_T} P, \qquad\qquad k_T = k_C$$

The additional degrees of freedom in the latter model (i.e., initiation/branching activation energies and cross-over temperatures) allows for increased flexibility to reproduce more complex chemical behaviors. Finally, the reactive mixture is assumed to have a constant mean molar mass, $\overline{W}$, and ratio of specific heats, $\gamma = c_p/c_v$, when modeled with the simplified schemes; see [9] for further details.

3 $D - \kappa$ curves

Figure 1 (left) shows the $D - \kappa$ curves obtained for a stoichiometric H_2-O_2 mixture at ambient pressure and temperature using the chemical models described above, and the same kinetic parameters as in Taileb et al. [9]: $A_s = 1.1 \times 10^9$ s^{-1} , and $E_a/R_u = 11277$ K, for single step; and $k_C = 2 \times 10^7$ s^{-1}, $E_I/R_u = 25000$ K, $E_B/R_u = 9300$ K, $T_I = 2431$ K, $T_B = 1430$ K, for three-step chain-branching chemistry. The mixture is characterized by γ and the total heat release, Q, whose values are given in Table 1.
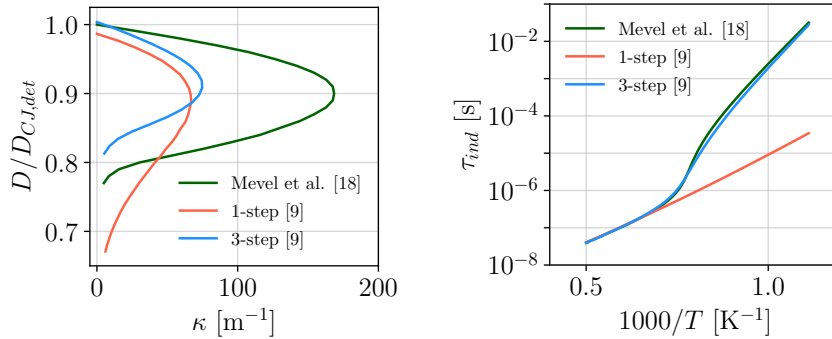

Figure 1: $D - \kappa$ curves (left) and constant volume induction times, τ_{ind} (right) at ρ_{vN} obtained with detailed kinetics [18] and simplified kinetics. $D_{\text{CJ, det}}$ is the steady propagation velocity computed with detailed chemistry. Conditions: stoichiometric H_2-O_2 at $p_0 = 100$ KPa and $T_0 = 300$ K.

Figure 1 clearly shows that simplified mechanisms fitted to reproduce the constant volume induction times of detailed kinetics, as was done in [9], yield significantly different turning points (i.e., κ_{crit}). More interesting is the fact that the κ_{crit} obtained ($\kappa_{\text{crit, 1-step}} = 67.4$ m^{-1}; $\kappa_{\text{crit, 3-step}} = 74.8$ m^{-1}; $\kappa_{\text{crit, det}} = 168.5$ m^{-1}) follows the same trend as that of the 2-D simulations of Taileb et al. [9] where the critical reactive layer heights, h_{crit}, for detonation propagation under yielding confinement were determined; a higher critical front curvature yields a lower h_{crit}. To compare with their results we use a crude estimate for the curvature

Table 1: Detonation and thermodynamic properties for a stoichiometric H_2-O_2 mixture for all chemical models used. The pre-exponential factors for simplified kinetics are also shown. Initial conditions: $p_0 = 100$ kPa and $T_0 = 300$ K.

	D_{CJ} [m/s]	T_{vN} [K]	$\gamma \, (0 - \mathrm{vN} - \mathrm{CJ})$	Q [MJ/kg]	A_s ; k_C [s^{-1}]	l_{ind} [μm]
Mevel et al. [18]	2839.9	1768.7	1.4 - 1.315 - 1.218	-	-	41
1-step [9]	2801.5	1674.8	1.33	4.800	6.0×10^9	87.9
New 1-step	2836.9	1769.5	1.35	4.606	1.08×10^{10}	36.2
3-steps [9]	2850.4	1723.7	1.33	4.990	2.0×10^7	46.8
New 3-steps	2836.2	1768.7	1.35	4.613	4.0×10^7	21.4

defined as $\kappa_{\mathrm{eq}} \propto 1/h_{\mathrm{crit}}$: $\kappa_{\mathrm{eq, 1\text{-}step}} = 41.7$ m^{-1}; $\kappa_{\mathrm{eq, 3\text{-}step}} = 50.0$ m^{-1} $\kappa_{\mathrm{eq, detailed}} = 166.7$ m^{-1}. Note that in both cases, $\kappa_{\mathrm{1\text{-}Step}} < \kappa_{\mathrm{3\text{-}step}} \ll \kappa_{\mathrm{Detailed}}$. This last observation may imply that using κ_{crit} as a fitting target for the development of simplified schemes could yield improved predictive capabilities in multidimensional simulations.
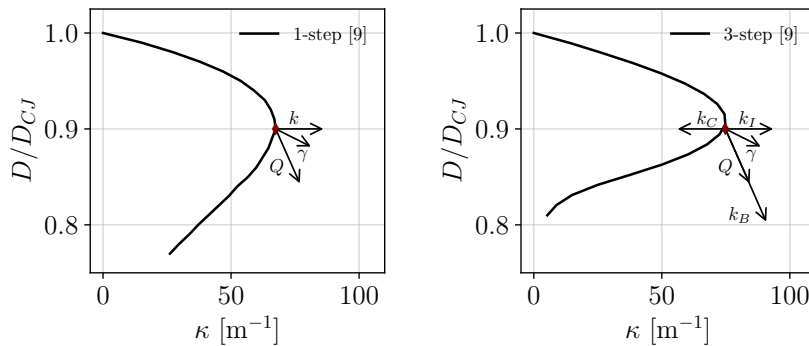
4 Fitting methodology

Figure 2: Influence of the thermodynamic and kinetic parameters on the calculated $D - \kappa$ curves for single-step (left) and three-step chain-branching kinetics (right). The size of the arrows indicates how sensitive the curve is to changes in each parameter.

Figure 2 shows the effect of varying the thermodynamic and kinetic parameters of the simplified schemes on the resulting $D - \kappa$ curves. The size of the arrows indicates how sensitive the curve is to changes in each parameter. For the modified mechanisms we chose to improve our initial conditions by matching as best as possible the steady detonation velocity, D_{CJ}, and von Neumman temperature, T_{vN}, computed with detailed kinetics. This entailed finding the best combination of Q and γ while ensuring that we were able to capture the proper velocity deficits for increasing κ, as well as the curve's turning point, κ_{crit}.

The parameters found after the fitting exercise are included in Table 1, and the updated $D - \kappa$ curves are shown in Fig. 3-left. Note that only A_s and k_C were modified and the initiation/branching activation energies and cross over temperatures were left unchanged. In agreement with the large activation energy asymptotics in [15]: (i) given fixed thermodynamic conditions and E_a/R_u, higher k results in larger κ_{crit}

values; (ii) an increase in T_{vN}, given by the new thermodynamics (i.e., Q and γ), yields a decrease in $D(\kappa_{\mathrm{crit}})$ and an increment in κ_{crit}. While both simplified schemes reproduce quite well the expected behavior for $D/D_{\mathrm{CJ, det}} > D/D_{\mathrm{CJ, det}}(\kappa_{\mathrm{crit}})$ significant deviations are present for larger deficits. The differences in the computed values of κ using detailed/three-step chain-branching kinetics when compared with those of single-step for $D/D_{\mathrm{CJ, det}} < 0.9$ are a consequence of the known inability of the single step model to adequately reproduce the H_2-O_2 ignition delay times at post-shock temperatures below the chain-branching cross-over temperature (see Fig. 3- right). Nonetheless, we speculate that this may not be a first order effect for accurately predicting h_{crit} in multidimensional simulations; capturing κ_{crit} may suffice.
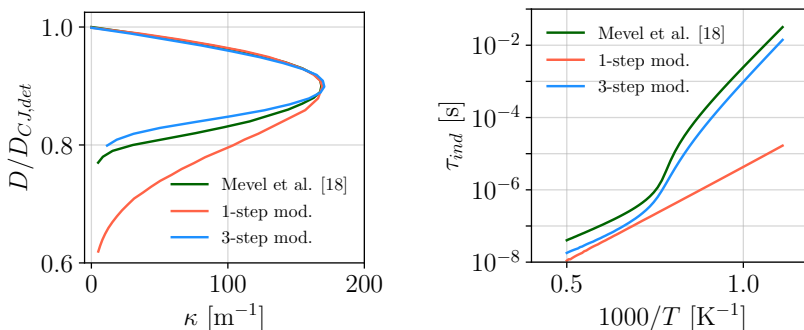

Figure 3: $D - \kappa$ curves (left), and constant volume induction times, τ_{ind} (right) at ρ_{vN} obtained with the modified simplified schemes compared with detailed kinetics results. Conditions: stoichiometric H_2-O_2 at $p_0 = 100$ KPa and $T_0 = 300$ K.

5 Conclusion

A methodology to develop simplified kinetic schemes was presented in which $D - \kappa$ curves obtained with detailed kinetics are used as the fitting target, aiming to capture the turning point of the curve, κ_{crit}. The updated schemes developed here are currently being used to determine h_{crit} using the same configuration of Taileb et al. [9] to test whether our hypothesis is valid. We will report our findings at the meeting.

Acknowledgements

References

[1] H. Wang, E. Dames, B. Sirjean, D. Sheen, R. Tangko, A. Violi, J. Lai, F. Egolfopoulos, D. Davidson, R. Hanson *et al.*, "A high-temperature chemical kinetic model of n-alkane (up to n-dodecane), cyclohexane, and methyl-, ethyl-, n-propyl and n-butyl-cyclohexane oxidation at high temperatures," *JetSurF version*, vol. 2, no. 2, p. 19, 2010.

[2] J. Van Oijen, F. Lammers, and L. De Goey, "Modeling of complex premixed burner systems by using flamelet-generated manifolds," *Combustion and Flame*, vol. 127, no. 3, pp. 2124–2134, 2001.

[3] P. Pepiot and H. Pitsch, "Systematic reduction of large chemical mechanisms," in *4th joint meeting of the US Sections of the Combustion Institute, Philadelphia, PA*, 2005, pp. 324–330.

[4] J. J. Hernández, R. Ballesteros, and J. Sanz-Argent, "Reduction of kinetic mechanisms for fuel oxidation through genetic algorithms," *Mathematical and Computer Modelling*, vol. 52, no. 7-8, pp. 1185–1193, 2010.

[5] S. Coronel, J. Melguizo-Gavilanes, D. Davidenko, R. Mével, and J. Shepherd, "Reduction methodology for detailed kinetic mechanisms: application to n-hexane-air hot surface ignition," in *Asia Pacific Combustion Conference*, vol. 11, 2017.

[6] A. Felden, L. Esclapez, E. Riber, B. Cuenot, and H. Wang, "Including real fuel chemistry in les of turbulent spray combustion," *Combustion and Flame*, vol. 193, pp. 397–416, 2018.

[7] W. Zheng, C. Kaplan, R. Houim, and E. Oran, "Flame acceleration and transition to detonation: Effects of a composition gradient in a mixture of methane and air," *Proceedings of the Combustion Institute*, vol. 37, no. 3, pp. 3521–3528, 2019.

[8] M. Kaneshige and J. E. Shepherd, "Detonation database," 1997.

[9] S. Taileb, J. Melguizo-Gavilanes, and A. Chinnayya, "Influence of the chemical modeling on the quenching limits of gaseous detonation waves confined by an inert layer," *Combustion and Flame*, vol. 218, pp. 247–259, 2020.

[10] J. Melguizo-Gavilanes, V. Rodriguez, P. Vidal, and R. Zitoun, "Dynamics of detonation transmission and propagation in a curved chamber: a numerical and experimental analysis," *Combustion and Flame*, vol. 223, pp. 460–473, 2021.

[11] B. Varatharajan, M. Petrova, F. Williams, and V. Tangirala, "Two-step chemical-kinetic descriptions for hydrocarbon–oxygen-diluent ignition and detonation applications," *Proceedings of the Combustion Institute*, vol. 30, no. 2, pp. 1869–1877, 2005.

[12] M. Short and J. J. Quirk, "On the nonlinear stability and detonability limit of a detonation wave for a model three-step chain-branching reaction," *Journal of Fluid Mechanics*, vol. 339, pp. 89–119, 1997.

[13] Z. Liang and L. Bauwens, "Cell structure and stability of detonations with a pressure-dependent chain-branching reaction rate model," *Combustion Theory and Modelling*, vol. 9, no. 1, pp. 93–112, 2005.

[14] Z. Liang, S. Browne, R. Deiterding, and J. Shepherd, "Detonation front structure and the competition for radicals," *Proceedings of the Combustion Institute*, vol. 31, no. 2, pp. 2445–2453, 2007.

[15] R. Klein, J. C. Krok, and J. Shepherd, "Curved quasi-steady detonations: Asymptotic analysis and detailed chemical kinetics," 1995.

[16] S. Browne, J. Ziegler, and J. Shepherd, "Numerical solution methods for shock and detonation jump conditions," *GALCIT report FM2006*, p. 90, 2008.

[17] D. G. Goodwin, R. L. Speth, H. K. Moffat, and B. W. Weber, "Cantera: An object-oriented software toolkit for chemical kinetics, thermodynamics, and transport processes," https://www.cantera.org, 2021, version 2.5.1.

[18] R. Mével, J. Sabard, J. Lei, and N. Chaumeix, "Fundamental combustion properties of oxygen enriched hydrogen/air mixtures relevant to safety analysis: Experimental and simulation study," *International Journal of Hydrogen Energy*, vol. 41, no. 16, pp. 6905–6916, 2016.